# METHOD OF EVALUATING HORIZONTAL AND VERTICAL EARTHQUAKE GROUND MOTIONS FOR ASEISMIC DESIGN

SUSUMU OHNO
Kajima Technical Research Institute, Kajima Corporation, 2-19-1, Tobitakyu, Chofu, Tokyo 182, Japan

TAKAAKI KONNO
Nuclear Structures Engineering Department, Kajima Corporation, 6-5-30, Akasaka, Minato-ku, Tokyo 107, Japan

KEN'ICHI ABE
Kumagai-Gumi Corporation, 2-1, Tsukudo-cho, Shinjuku-ku, Tokyo 162, Japan

TORU MASAO
Tajimi Engineering Services Ltd., 3-2-26, Nishi-Shinjuku, Shinjuku-ku, Tokyo 160, Japan

SETSUO IIZUKA and HIROTOSHI UEBAYASHI
Siting Technology Department, Nuclear Power Engineering Corporation, 4-3-13, Toranomon, Minato-ku, Tokyo 105, Japan



## ABSTRACT

Using earthquake records from California, Funaoka array records from Japan, and records of recent great earthquakes in Japan and Mexico, relations between horizontal and vertical components in terms of response spectra and time envelopes are investigated. Vertical-to-horizontal spectral ratios on soft rock are estimated for the portion after arrival of the initial S-wave. Jennings-type envelopes are fitted to observation records and the envelopes are modeled by functions of magnitude and source-to-site distance. The durations of the vertical components are almost the same as those of horizontal components except the vertical component builds up faster than horizontal components. Based on these results, the horizontal-to-vertical spectral transfer coefficient and the time envelopes of horizontal and vertical motions are established for use in aseismic design.

## KEYWORDS

Vertical Motion; Envelope Function; Design Spectrum; Artificial Earthquake Motion

## OBJECTIVE

Methods of evaluating earthquake motion for the aseismic design of nuclear power plants have been established and applied to practical use with regard to horizontal components, but are still being investigated with regard to vertical components. The objective of this paper is to establish a reasonable method of evaluating for aseismic design not only horizontal but also vertical earthquake motions by investigating recent earthquake records.

## DATA

The data used in this analysis consist of three different data sets as follows.

Data set C comprises 272 horizontal and 136 vertical USGS or CDMG strong-motion components of 12 earthquakes in California. Magnitude and shortest distance from the fault range from 5.0 to 7.5 and from 1 to 50 km, respectively. Thirty-two records were collected on rock and 104 records on soil. The S-wave

velocities ($V_s$) of the rock sites are distributed above 600 m/s.

Data set F comprises 224 horizontal and 112 vertical Funaoka array (KASSEM; Shimizu *et al.*, 1988; Abe *et al.*, 1990) strong-motion components of 22 earthquakes along the Pacific coast of Japan. Magnitude and epicentral distance range from 4.6 to 6.1 and from 100 to 200 km, respectively. The Funaoka array comprises 7 surface sites and 1 vertical array (6 seismometers); geologically, the sites are located from basement (granodiorite) to recent alluvium.

Data set G comprises 38 horizontal and 19 vertical components of recent great earthquakes and their aftershocks in Japan and Mexico. These are: 1983 Japan Sea (*M*7.7) and its largest aftershock (*M*7.1), 1985 Michoacan (*M*8.1) and its largest aftershock (*M*7.5), 1993 Kushiro-oki (*M*7.8), 1993 Hokkaido-Nansei-oki (*M*7.8) and its largest aftershock (*M*6.3). Many sites are on rock or hard soil.

Figure 1 shows epicenters for the three data sets. Figure 2 shows distribution of magnitudes and source-to-site distances for the data sets. The portion after the time-integration of the square sum of two horizontal components becomes 5% is used for data set C, and the portion after the initial S-wave arrival, which is defined visually, is used for data sets F and G. These procedures are taken to eliminate P-waves (which arrive directly from the fault before S-waves) from the vertical components, and to use the main portions of the horizontal components for analysis.

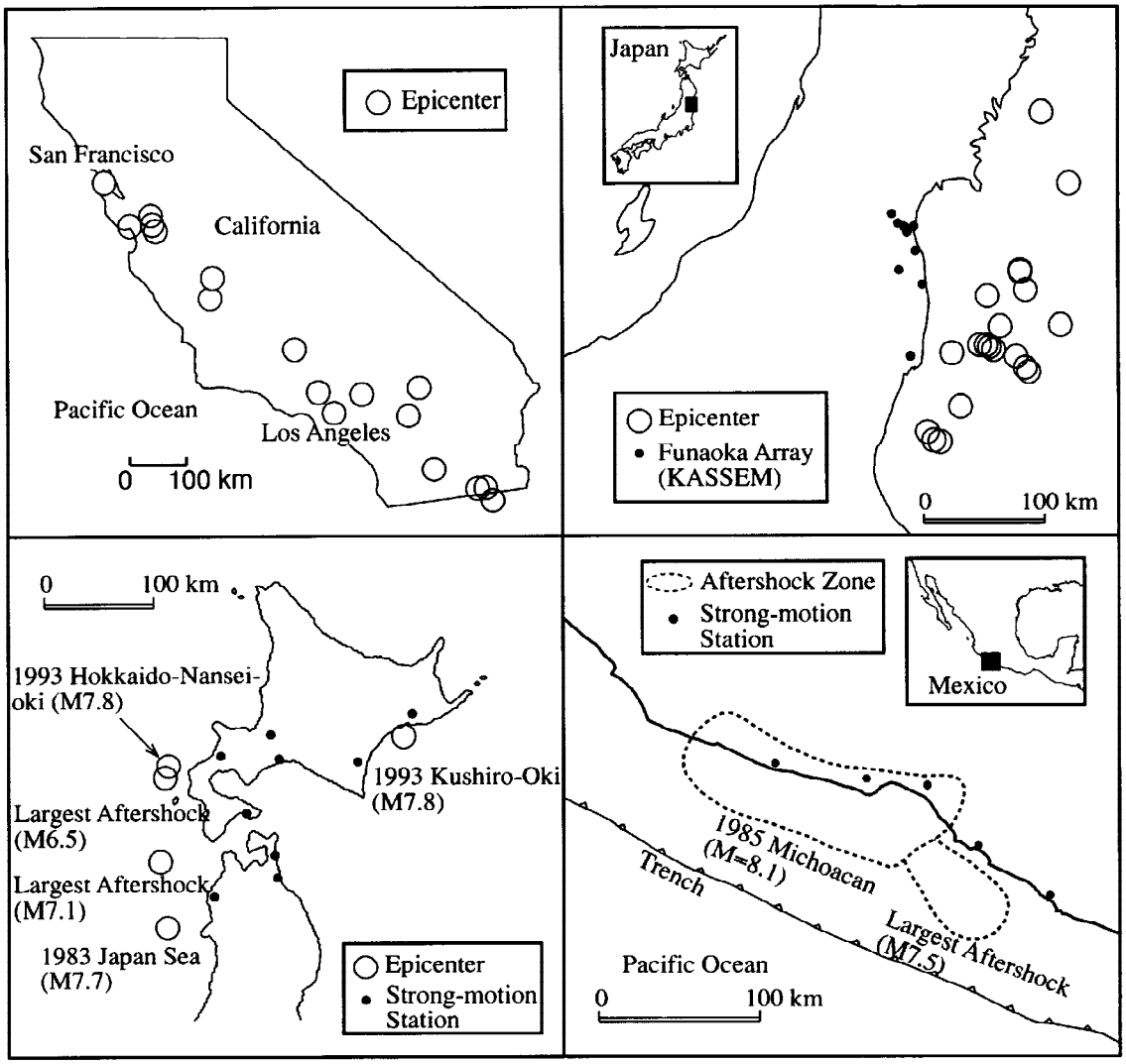


Fig. 1 Epicenters of California data earthquake (top left), Funaoka array data earthquake (top right), recent great earthquake in Japan (bottom left) and recent great earthquakes in Mexico (bottom right).

## VERTICAL-TO-HORIZONTAL RESPONSE SPECTRAL RATIOS

Following Takemura *et al.* (1987), 5%-damping response spectrum $S(T)$ is modeled as

$$\log S(T) = a(T)M - \log X - b(T)X + \delta_i\, c_i(T) \qquad (1)$$

where $T$ is period, $M$ is magnitude, $X$ is source-to-site distance, and $\delta_i$ is a dummy variable to stratify the site condition. The sites are stratified by rock and soil for data set C, and stratified by station for data set F. The coefficients $a(T)$, $b(T)$, $c_i(T)$ are estimated by regression analysis of the response spectra of horizontal and vertical records. For data set F, hypocentral distance is used as source-to-site distance $X$, while Equivalent Hypocentral Distance $X_{eq}$ (distance from a virtual point source that radiates the same energy as a finite-sized fault; Ohno *et al.*, 1993) is used for data set C because many near-source data are included.

For the portion after the initial S-wave arrival, the effects on horizontal and vertical components of source (earthquake causative fault) and propagation path from the source to the basement below the site are expected to be the same. However, as the horizontal components propagate mainly as S-waves and the vertical components propagate mainly as P-waves above the basement (Takahashi *et al.*, 1992), the difference in horizontal and vertical components must appear in the site factor.

Regression analyses of response spectra were conducted independently for horizontal and vertical components in data set F. As predicted above, the estimates of $a(T)$ and $b(T)$ are very similar, while the site-coefficients $c_i(T)$ are different between horizontal and vertical components. Based on these results, the values of $a(T)$ and $b(T)$ for the vertical component are set to be identical for horizontal components in data set C. Consequently, the relation between response spectra of horizontal and vertical components is independent of $M$ and $X$, and can be represented as the ratio between these response spectra.

Figure 3 shows the vertical-to-horizontal spectral ratios calculated from the regression coefficients for the California rock sites (Vs ≥ 600 m/s) and the Funaoka array S2-site (Vs = 700 m/s). The spectral ratios of data set C and data set F have similar characteristics.

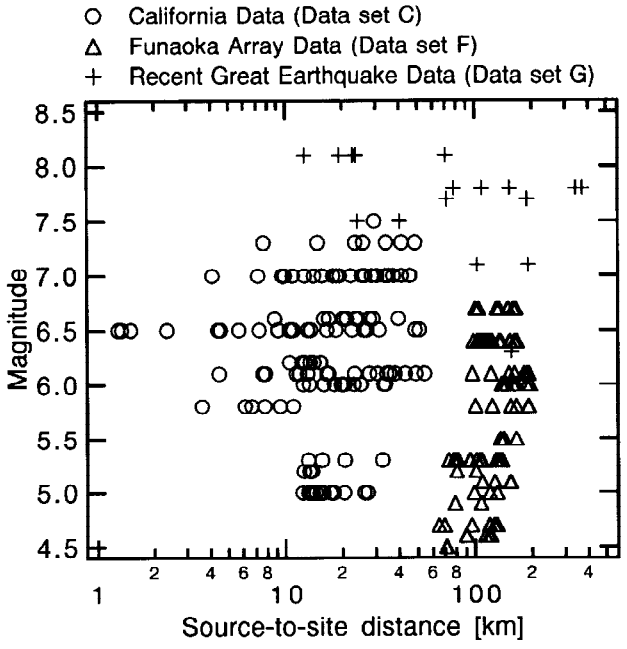


Fig. 2 M-X distributions of the California, the Funaoka array, and the recent great earthquake data.

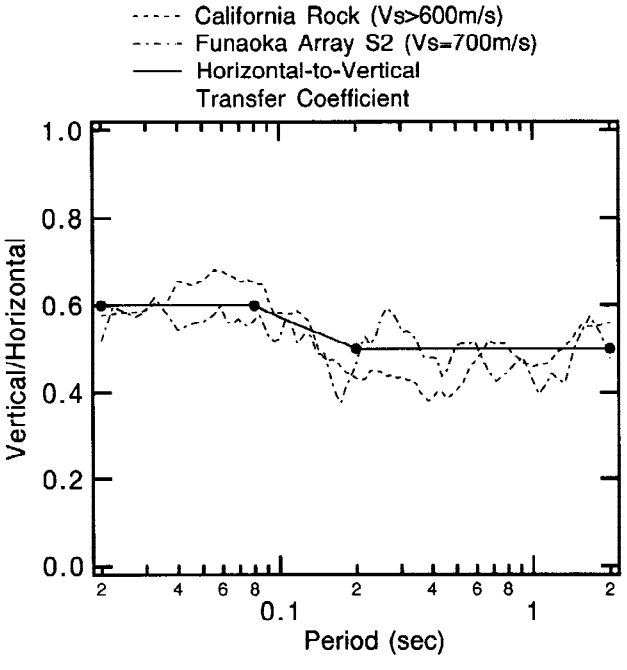


Fig. 3 Vertical-to-horizontal spectral ratios evaluated from the California and the Funaoka array data. The horizontal-to-vertical spectral transfer coefficients are also shown.

## Time Envelope Fitting and Modeling of Envelope Duration

As in Jennings *et al.* (1969), time envelope $E(t)$ is modeled by a combination of three segments as follows:

$$E(t)=\begin{cases} A(t/t_b)^2 & (t \le t_b) \\ A & (t_b \le t \le t_c) \\ A\exp\left[\ln(0.1)(t-t_c)/(t_d-t_c)\right] & (t_c \le t \le t_d) \end{cases} \quad (2)$$

where $t$ is time. The first segment is the build-up in quadratic form, the second segment is the central segment with constant amplitude, and the third segment is the coda with exponential decay. $t_d$ is defined as the time when $E(t_d)=A/10$. $A$, $t_b$, $t_c$, $t_d$ are estimated using the least-squares method of Dan and Watanabe (1989) to make equation (2) fit observation records . Figure 4 shows an example of fitting.

As for data set C, the estimates of $t_b$ are widely scattered and are sometimes zero. This is probably because the analysis was done on the portion after the time-integration of the square sum of two horizontal components becomes 5%, and the true initial S-wave arrival may have been lost. Therefore $t_c$ is directly estimated instead of $t_b$ and $t_c$-$t_b$ for data set C.

As $t_b$ and $t_c$ have strong correlation with $M$ but weak correlation with $X$, durations $t_b$, $t_c$, and $t_c$-$t_b$ are modeled as a linear equation of $M$. On the other hand, as $t_d$-$t_c$ has strong correlation with both $M$ and $X$, $t_d$-$t_c$ is modeled by a linear combination of $M$ and log$X$. Because it is better that the data used in the regression analysis have uniform distribution of $M$ and $X$, data set G is added to both data set C and data set F. For data sets C and G, segments of the envelope of horizontal components are estimated as:

$$\log t_c = 0.397M - 1.774, \quad (3)$$

$$\log(t_d - t_c) = 0.011M + 0.133\log X_{eq} + 1.023, \quad (4)$$

and the estimates of horizontal components for data sets F and G are:

$$\log t_b = 0.242M - 1.282, \quad (5)$$

$$\log(t_c - t_b) = 0.193M - 0.588, \quad (6)$$

$$\log(t_d - t_c) = 0.115M + 0.176\log X + 0.162. \quad (7)$$

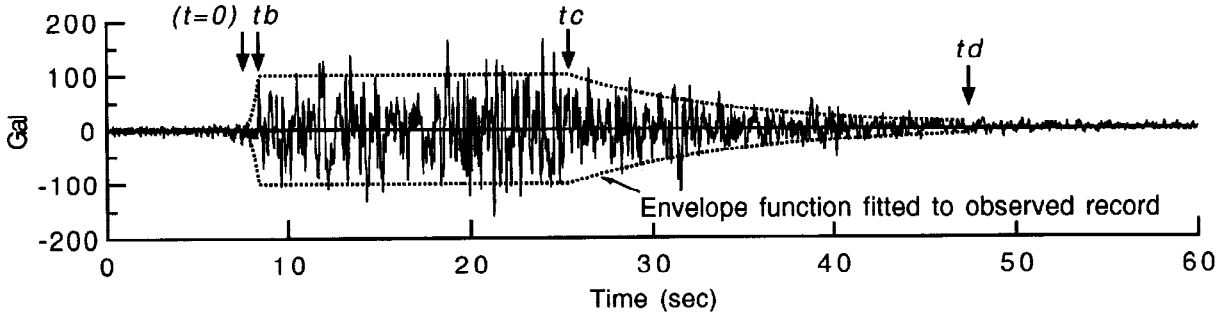


Fig. 4 An example of time envelope fitted to an observed record (Michoacan earthquake, La Union, NS Component)

## Building-up and Central Segments

The chart on the left in Fig. 5 shows the estimates of $t_c$ versus $M$. The estimates for data set F only are also plotted for comparison. $t_c$ is regarded as apparent rupture duration $\tau$, which is the time difference between the first and the last arrivals of direct S-waves radiated from the earthquake fault (Takemura *et al.*, 1989; Dan and Watanabe, 1989) as:

$$\tau=L(1/V_r-\cos\theta/\beta) \tag{8}$$

where $L$ is fault length, $V_r$ is rupture velocity, $\beta$ is S-wave velocity of the propagation path, and $\theta$ is the angle between the site and the rupture starting point. In Fig. 5, minimum and maximum values of $\tau$ are plotted under the condition that $\log L=0.5M-1.88$ (Sato, 1979), $V_r$=2.8 km/s, $\beta$=3.5 km/s, $\theta$=0° and 180°. The estimates generated by this analysis are located between the maximum and minimum and are thus within the range predicted by the fault model.

The estimates for data set F only are smaller than those for data sets F and G at small magnitudes, and are larger at large magnitudes. This is because the durations of data set G are smaller than would be expected based on data set F, that is, the actual durations of earthquake motions at large magnitudes are smaller than the results of extrapolating from small magnitudes. The same tendency exists between data set C and data set G. This is probably because multiple peaks generally appear in the waveforms of large earthquakes and central part of the envelope is fitted to only one of the peaks, while single peaks are common for small earthquakes and are well represented by the envelope described by equation (2).

Compared with the estimates for data sets C and G, the estimates for data sets F and G are relatively larger at $M$<6.5 and smaller at $M$>6.5. As the same data set (data set G) is used at large magnitudes, these differences are due to differences between data set C and data set F. For engineering purposes, differences at small magnitudes are not so significant, but such data set-dependency as well as the effect of multiple peaks at large magnitudes may need further investigation.

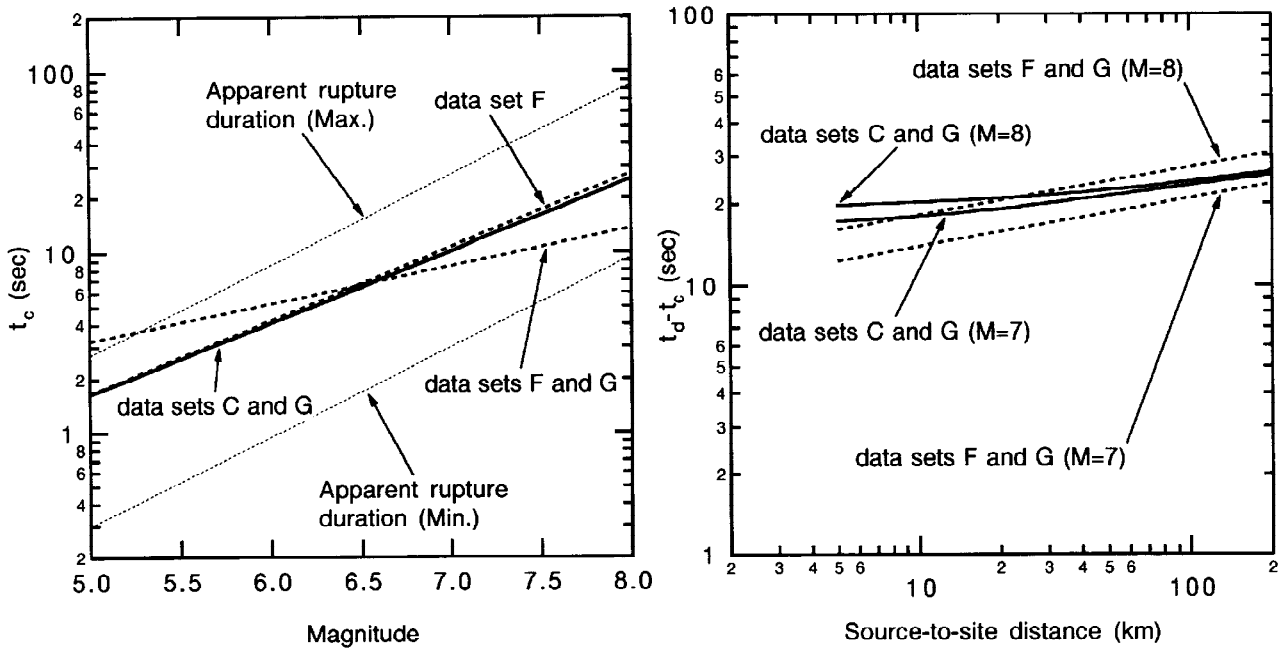


Fig. 5 Estimated durations of the envelopes of horizontal components. The central part (left) and the coda part (right).

## Coda Segment

The right side of Fig. 5 shows the estimates of $t_d$-$t_c$ versus $X$ for $M$=7 and $M$=8. As used in the analysis of response spectrum, $X_{eq}=R/\{\ln[1+(R/X)^2]\}^{0.5}$, $R=10^{0.5M-2.28}$ is used for data sets C and G under the assumption that the fault is circular with radius $R$ and that the site is located on the orthogonal central axis of the fault at distance $X$ (Ohno *et al.*, 1993). Although the estimated coefficients of equation (4) and equation (7) are slightly different, the estimated durations are in agreement.

## Relation between Horizontal and Vertical Components

Figure 6 shows the relation between estimated durations of horizontal and vertical components for data sets F and G. The vertical component durations are almost the same as the horizontal component durations for the central and coda segments, while the vertical component durations are smaller than the horizontal component durations for the build-up segment. This faster build-up of the vertical component is probably due to differences in P- and S-wave behavior above the basement, and, to some extent, contamination by the tail of direct P-waves from the source. The estimate of $t_b$ for the vertical component is:

$$\log t_b=0.215M-1.381. \tag{9}$$

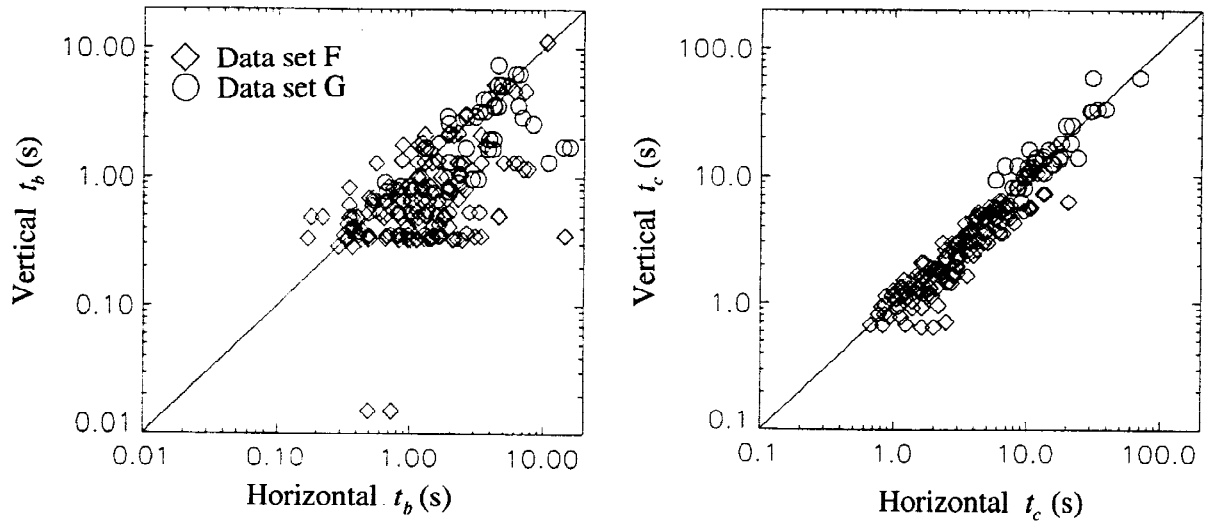


Fig. 6 Relation between durations of horizontal and vertical envelopes for the Funaoka array data and the great earthquake data (data sets F and G).

## ARTIFICIAL EARTHQUAKE MOTION FOR ASEISMIC DESIGN

Based on the estimated vertical-to-horizontal spectral ratios (dashed lines in Fig. 3), the horizontal-to-vertical spectral transfer coefficient is established as the straight line in Fig. 3. The spectral transfer coefficient is 0.6 for short periods ($0.02<T<0.08$ s) and 0.5 for long periods ($0.2<T<2.0$ s), and is calculated by log-log interpolation for medium periods ($0.08<T<0.2$ s). As described above, the relation between the response spectra of horizontal and vertical components could depend on site condition. As S-wave velocities of the California rock sites are more than 600 m/s, and that of the Funaoka array S2 site is 700 m/s, this transfer coefficient is established mainly for soft rock with $V_s\approx$700 m/s and attention would be necessary when being applied to different site conditions.

Envelope functions of horizontal motions are established by the average between the estimates for data sets C and G and those for data sets F and G, except that equation (5) is just used for $t_b$. The envelope of the vertical components is established to be the same as that of the horizontal components, while equation (9) is

used for $t_b$ to represent the faster build-up of vertical components.

Following the above method, response spectra and time envelopes of horizontal and vertical components are created for $M$=7.0, epicentral distance $\Delta$=20 km as an example. The horizontal response spectrum is established by the method of Hisada *et al.* (1978) under the assumption that focal depth $H$ is

$$\log H = 0.353M - 1.435. \tag{10}$$

The vertical response spectrum is obtained by multiplying the horizontal spectrum by the above horizontal-to-vertical spectral transfer coefficient. Sine-wave synthesis is used to create an artificial wave $f(t)$ :

$$f(t) = E(t)\sum_{i=0}^{N-1} A_i \cos(\omega_i t + \phi_i) \tag{11}$$

where $N$ is number of data ($N=t_d/\Delta t$; sampling time $\Delta t$=0.01s), $\omega$ is circular frequency and $\phi_i$ is random phase ($0<\phi_i<2\pi$). $f(t)$ is made to satisfy the following conditions:

Spectral Ratio: $\varepsilon(T)=SA_1(T)/SA_2(T) \geq 0.85, \quad (0.02 \leq T \leq 2.0)$ (12)

Spectrum Intensity Ratio: $\int_{0.1}^{2.5} Sv_1(T)dt \Big/ \int_{0.1}^{2.5} Sv_2(T)dt \geq 1.0$ (13)

Coefficient of Variation: $V_\varepsilon \leq 0.05, \quad (0.04 \leq T \leq 2.0)$ (14)

Error: $|1-\bar{\varepsilon}| \leq 0.02, \quad (0.04 \leq T \leq 2.0)$ (15)

where suffixes 1 and 2 indicate target spectrum and spectrum of artificial wave, respectively. $SA$ and $Sv$ are acceleration and pseudo-velocity response spectra with 5% damping, respectively. $\varepsilon$ is average of $\varepsilon(T)$ over the period range and $V_\varepsilon$ is coefficient of variation (COV) of $\varepsilon(T)$. Artificial earthquake motions which satisfy the above conditions are shown in Fig. 7 with the horizontal and vertical response (target) spectra and the time envelopes.

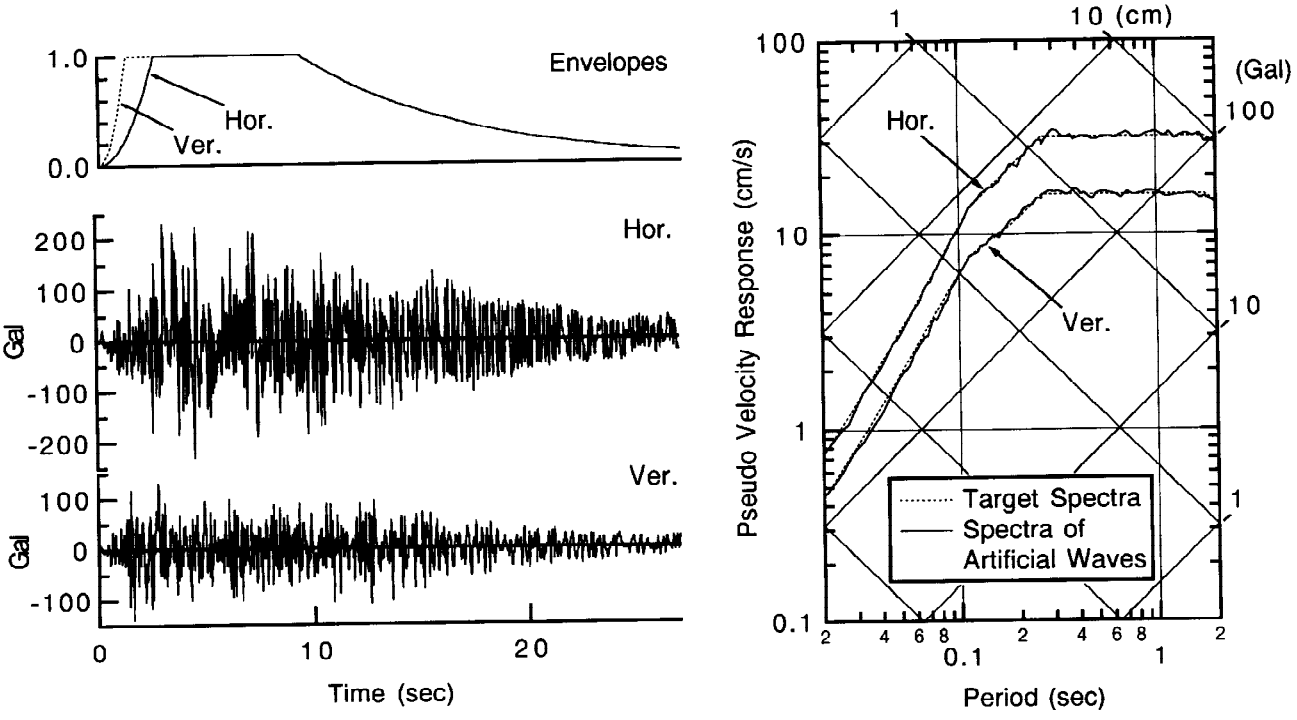


Fig. 7 An example of time histories and response spectra of horizontal and vertical artificial earthquake motions established in this study for use of aseismic design. (M=7.0, Δ=20 km)

## CONCLUSIONS

Using earthquake records from California, Funaoka array records from Japan, and records of recent great earthquakes in Japan and Mexico, the horizontal-to-vertical spectral transfer coefficient on soft rock (Vs≈700 m/s) and horizontal and vertical time envelopes are established. The spectral transfer coefficient is 0.6 for short periods (≤0.08 s) and 0.5 for long periods (≥0.2 s). The durations of the vertical components are almost the same as those of horizontal components except that the vertical components build up faster than the horizontal components. Being based on the analysis of recent earthquake records and considering both horizontal and vertical components, these results are considered appropriate to prescribe earthquake motions used for aseismic design. As further researches, some major issues remain to be investigated. These are the effects of direct P-wave, the envelope modeling for multiple shocks, and dealing of the variation from median value.

## ACKNOWLEDGMENTS

This work was carried out by NUPEC as a project sponsored by the Ministry of International Trade and Industry of Japan. This work was reviewed by "Committee of Advanced Seismic Design for LWR" of NUPEC. The authors wish to express their gratitude for the cooperation and valuable suggestions given by every committee members.

## REFERENCES

Abe, K., K. Kasuda, M. Terada, and T. Shimizu (1990) Characteristics of vertical earthquake motions obtained from the dense instrument array observation system KASSEM, Proc. 8th Japan Earthq. Eng. Symposium, 481-486.

Dan, K. and T. Watanabe (1989) A study on envelope functions of earthquake ground motions, Summaries of Technical papers of Annual Meetings of A.I.J., 773-774 (in Japanese).

Hisada, T., Y. ohsaki, M. Watabe, and T. Ohta (1978) Design spectra for stiff structures on rock, Proc. 2nd Int. Conf. on Microzonation, 1187-1198.

Jennings, P. C., G. W. Housner, and N. C. Tsai (1969) Simulated earthquake motions for design purposes, Proc. 4th World Conf. Earthq. Eng., 145-160.

Ohno, S., T. Ohta, T. Ikeura., and M. Takemura (1993) Revision of attenuation formula considering the effect of fault size to evaluate strong motion spectra in near field, Tectonophys. 218, 69-81.

Sato, R. (1979) Theoretical basis on relationships between focal parameters and earthquake magnitude, J. Phys. Earth, 27, 353-372.

Shimizu, T., K. Abe, K. Kasuda and E. Yanagisawa (1988). The development of the dense instrument array system KASSEM and the analysis of observed earthquake waves. Proc. 9th World Conf. Earthq. Eng., VIII-137-142.

Takahashi, K., S. Ohno, M. Takemura, T. Ohta, T. Hatori, Y. Sugawara, and S. Omote (1992) Observation of earthquake strong-motion with deep borehole, Generation of vertical motion propagating in surface layers after S wave arrival, Proc. 11th World Conf. Earthq. Eng., 1245-1250.

Takemura, M., T. Ohta, and S. Hiehata (1987) Theoretical basis of empirical relations about response spectra of strong ground-motions. Journal of Struct. Constr. Engng., A.I.J., 375, 1-9 (in Japanese with English abstract).

Takemura, M., M. Kamata, and T. Kobori (1989) A method for stochastic prediction of strong ground motions on the basis of the theoretical seismic-wave radiation and propagation, Journal of Struct. Constr. Engng., A.I.J., 403, 25-34 (in Japanese with English abstract).